JOURNAL OF OPTIMIZATION THEORY AND APPLICATIONS: Vol. 52, No. 1, JANUARY 1987

A Differential Game of Surveillance Evasion of Two Identical Cars[1]

I. GREENFELD[2]

Communicated by J. V. Breakwell

Abstract. A partial solution of a differential game of surveillance evasion is presented. The dynamics is that of two identical cars, with constant speeds and bounded turn rates. The pursuer's surveillance zone is circular. The game of kind and the game of degree are solved for ratios of the surveillance radius to the minimal turn radius equal to or greater than $\pi + 2$. A barrier is constructed, and regions of strategies are separated through the use of dispersal and universal surfaces. A synthesis of a composite game of two identical cars is outlined, covering the space outside the surveillance zone as well as that inside it.

Key Words. Surveillance evasion, differential games, two identical cars, game of kind, game of degree.

1. Introduction

This paper treats a zero-sum, two-player, full-information differential game of surveillance evasion. The two identical cars' dynamics is used, and the game space is the radial zone of surveillance.

The model, though extensively simplified for reasons of convenience, represents a class of practical cases, whereby two similar vehicles have a relatively small ratio of surveillance radius to turn radius. Examples may be derived from maritime scenarios. Other applications such as collision avoidance may also be considered.

Only a few researches treated games of surveillance evasion. In this set of games, the pursuer's goal is holding the evader within a surveillance zone, rather than capturing the evader. Although the kinematics may be

[1] Part of this research (the game of kind, Ref. 1) was carried out in the Faculty of Mechanical Engineering in the Technion, Haifa under the supervision of J. Lewin. The author is indebted to J. Lewin for his guidance.

[2] Research Engineer, Armament Development Authority, Ministry of Defense, Israel.

0022-3239/87/0100-0053$05.00/0

identical, the two problems are essentially different, mainly by the definition of the game space and the players' objectives.

The game of pursuit of two identical cars was solved fully by Merz (Ref. 2). Due to the identical dynamics, it bears resemblance to this work. The homicidal chauffeur game of kind of surveillance-evasion was solved by Dobbie (Ref. 3). Lewin and Breakwell (Ref. 4) solved the game of degree of the same model, the solution being quite complicated. Lewin and Olsder (Ref. 5) solved the same dynamics for a conic surveillance zone.

This work presents a full solution of the surveillance evasion game of kind and degree of two identical cars with a radial surveillance zone, at part of the parametric space. The definition of the problem and the kinematics are presented in Section 2. Section 3 outlines the basic concepts of solution [using Isaacs' methods, (Ref. 6)] and the general equations of optimal paths. The game of kind and the construction of the barrier are presented in Section 4. The game of degree is presented in Section 5. Section 6 includes a comparison to the game of pursuit by Merz, and an attempt to synthesize a composite game of two identical cars.

2. Problem of Surveillance-Evasion

2.1. Definitions. The two players, a pursuer (or surveiller) P and an evader E, move in a two-dimensional realistic space. Their dynamics is identical, and consists of constant speed $W=1$ and minimal turn radius $R=1$. The turn rate is controlled by the control variables u and v of P and E, respectively. Both players have full information of the current state of the game, but no information as to the opponent's current control.

The pursuer has a surveilling device with a range of effectiveness of radius K. The game goes with the evader trying to get out of the surveillance zone within minimal time, while the pursuer wishes to prevent it or, if not possible, to prolong his surveillance for as long as possible. Finding their optimal strategies and the optimal paths is the essence of this work.

Two aspects of the solution will be discussed: The game of kind (GOK) where the barrier B, separating an escape zone EZ and a capture (or surveillance) zone CZ, is constructed; and the game of degree (GOD), where the regions of strategies and the optimal paths in the escape zone are found.

In the GOK, the barrier is constructed as a nonleaking semipermeable surface, by Isaacs' methods. The barrier strategies, u^* and v^*, and paths are defined.

In the GOD, the payoff is defined as the time to termination (escape) T_f, which P maximizes and E minimizes using their optimal strategies u^*

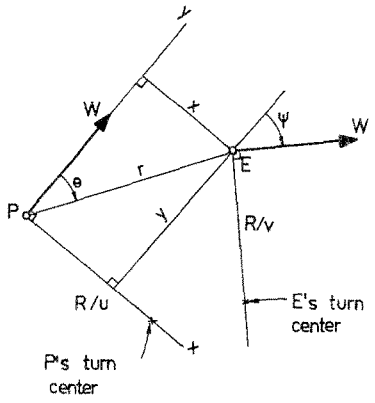

Fig. 1. Coordinate systems in the game of two identical cars.

and v^*, respectively. Thus, a saddle-point sufficiency condition is satisfied, and the value T (the time to go, under optimal play) is defined. The optimal strategies and paths are outlined by Isaacs' methods.

2.2. Coordinate Systems and Kinematic Equations. We shall use two coordinate systems to denote the relative position between the players: Cartesian (x, y, ψ) and polar (r, θ, ψ). See Fig. 1. They constitute a three-dimensional relative game space S (the state space) with a cylindrical boundary C (see Fig. 2),

$$x_c^2 + y_c^2 = k^2, \qquad 0 \leq \psi \leq 2\pi. \tag{1}$$

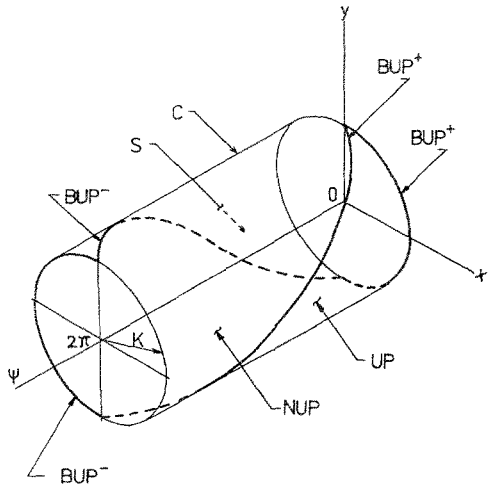

Fig. 2. Usable part and its boundaries.

The dimensionless kinematic equations of the two identical cars' dynamics shall be, using retrograde time $\tau(\tau \equiv T_f - t;\ \mathring{x} = -\dot{x})$,

$$\mathring{x} = -\sin\psi + uy, \tag{2a}$$

$$\mathring{y} = -\cos\psi + 1 - ux, \tag{2b}$$

$$\mathring{\psi} = u - v, \tag{2c}$$

with

$$|u| \leq 1, \qquad |v| \leq 1. \tag{2d}$$

The vectograms of the game are convex, which implies extremal controls. Yet, they are not strictly convex; thus, intermediary values are also possible.

The only parameter of the problem, in the dimensionless form, is K, which is the ratio of the surveillance radius to the minimal turn radius.

Termination is defined on the boundary C by

$$\mathring{r}_0 = -\cos(\psi_0 - \theta_0) + \cos\theta_0 < 0, \tag{3}$$

where the index 0 denotes initial conditions in the retrograde sense. The usable part UP is, therefore,

$$|\psi_0| < 2|\theta_0|, \tag{4}$$

and the boundaries of the usable part (BUP's) are the two spirals $\psi_0 = 2\theta_0$ and the two half-circles $\psi_0 = 0$, $r_0 = K$. Figure 2 depicts the BUP's on the boundary C, in the state space. On the figure, $(+)$ indicates right side $(\theta < \pi)$, and $(-)$ indicates left side $(\theta > \pi)$.

3. General Solutions for the Path Equations

3.1. Optimal Controls and Differential Equations. The necessary conditions consist of Isaacs' main equations (ME), the kinematic equations, the adjoint equations, and the control constraints. The necessary conditions yield a set of differential equations which is solved by retrograde integration, with initial conditions defined on the usable part.

The Hamiltonian H in the GOD is

$$H(X, \nabla T, u, v) = T_x\dot{x} + T_y\dot{y} + T_\psi\dot{\psi} + 1$$

$$= uA + vT_\psi + T_x\sin\psi + T_y\cos\psi - T_y + 1, \tag{5a}$$

$$A \equiv xT_y - yT_x - T_\psi, \tag{5b}$$

where $X \equiv (x, y, \psi)$ is the state vector and $\nabla T \equiv (T_x, T_y, T_\psi)$ is the gradient of the value T. The payoff integrand is 1.

Isaacs' ME1 is

$$\min_{|v|\le 1} \max_{|u|\le 1} H(X, \nabla T, u, v) = 0. \tag{6}$$

By optimizing, we get ME2 along an optimal path,

$$H^* \equiv H(X, \nabla T, u^*, v^*)$$
$$= |A| - |T_\psi| + T_x \sin\psi + T_y \cos\psi - T_y + 1 = 0, \tag{7}$$

which is satisfied by the candidates for optimal strategies u^* and v^*,

$$u^* = \operatorname{sign} A \equiv \sigma_1, \tag{8a}$$

$$v^* = \operatorname{sign}(-T_\psi) \equiv \sigma_2. \tag{8b}$$

Here, $\operatorname{sign}(\cdot)$ is the sign function, nondefined when the argument is zero. A and T_ψ are the switch functions of the controls of P and E, respectively.

The adjoint equations along an optimal path are

$$\mathring{T}_x = \partial H^*/\partial x = \sigma_1 T_y, \tag{9a}$$

$$\mathring{T}_y = \partial H^*/\partial y = \sigma_1 T_x, \tag{9b}$$

$$\mathring{T}_\psi = \partial H^*/\partial \psi = T_x \cos\psi - T_y \sin\psi. \tag{9c}$$

The adjoint equations are used to determine the values of the switch functions.

In the GOK, $\nu \equiv (\nu_x, \nu_y, \nu_\psi)$, the normal to the barrier, heading into the capture zone, substitutes ∇T in the equations, with a complete analogy in the solutions thereafter. Since there is no payoff in the GOK, the payoff integrand is zero, which renders a slight difference in the Hamiltonian. Therefore, ME2 in the GOK is

$$H^* \equiv H(X, \nu, u^*, v^*)$$
$$= |A| - |\nu_\psi| + \nu_x \sin\psi + \nu_y \cos\psi - \nu_y = 0. \tag{10}$$

3.2. Optimal Path Equations. The initial conditions at $\tau = 0$ (not necessarily on the boundary C), using a parametric form, are

$$X_0 = (r_0 \sin\theta_0, r_0 \cos\theta_0, \psi_0), \tag{11a}$$

$$\nabla T_0 = (s_1 \sin s_2, s_1 \cos s_2, T_{\psi 0}), \tag{11b}$$

the parameter vectors being (r_0, θ_0, ψ_0) and $(s_1, s_2, T_{\psi 0})$.

We present general solutions of the two cases encountered in this work: the case of extremal controls, whereby $\sigma_1, \sigma_2 = \pm 1$; and the case of zero control for E, whereby $\sigma_1 = \pm 1$ and $\sigma_2 = 0$.

The following equations are also valid for the GOK, with ∇T substituted by ν. The solution is attained by retrograde integration of the kinematic equations (2), with the controls (8), and of the adjoint equations (9), with the aid of ME2 (7). The initial conditions are (11).

The optimal path's general equations are given below.

Extremal Controls: $\sigma_1 = \pm 1$, $\sigma_2 = \pm 1$. The state vector X is given by

$$x = r_0 \sin(\theta_0 + \sigma_1 \tau) + \sigma_1 (1 - \cos \tau) + \sigma_2 [\cos(\psi_0 + \sigma_1 \tau) - \cos \psi], \tag{12a}$$

$$y = r_0 \cos(\theta_0 + \sigma_1 \tau) + \sin \tau - \sigma_2 [\sin(\psi_0 + \sigma_1 \tau) - \sin \psi], \tag{12b}$$

$$\psi = \psi_0 + (\sigma_1 - \sigma_2)\tau. \tag{12c}$$

The gradient of the value T is given by

$$T_x = s_1 \sin(s_2 + \sigma_1 \tau), \tag{13a}$$

$$T_y = s_1 \cos(s_2 + \sigma_1 \tau), \tag{13b}$$

$$T_\psi = T_{\psi 0} - s_1 \sigma_2 [\cos(\psi_0 - s_2 - \sigma_2 \tau) - \cos(\psi_0 - s_2)]. \tag{13c}$$

The switch functions are

$$A = r_0 s_1 \sin(\theta_0 - s_2) - T_{\psi 0} + \sigma_1 s_1 [\cos(s_2 + \sigma_1 \tau) - \cos s_2] \tag{14}$$

and T_ψ is as in (13).

Zero Control for E: $\sigma_1 = \pm 1$, $\sigma_2 = 0$. Assuming the existence of a singular optimal path created by $T_\psi = 0$, and using the property of continuity of ∇T across that path (due to convexity), we may find E's control by taking $\mathring{T}_\psi = 0$. Differentiating (13), we get $\sigma_2 = 0$. The validity of this assumption will be established later.

The state vector X for this case is

$$x = r_0 \sin(\theta_0 + \sigma_1 \tau) - \tau \sin \psi + \sigma_1 (1 - \cos \tau), \tag{15a}$$

$$y = r_0 \cos(\theta_0 + \sigma_1 \tau) - \tau \cos \psi + \sin \tau, \tag{15b}$$

$$\psi = \psi_0 + \sigma_1 \tau. \tag{15c}$$

T_x and T_y are the same as in (13), while $T_\psi = 0$. The switch function A is the same as in (14).

4. Game of Kind (GOK): Construction of the Barrier

4.1. General Concepts. We look for a composite, closed, nonleaking barrier B, dividing the game space into an escape zone EZ and a capture zone CZ. The existence of such a barrier may be demonstrated by observing that some initial conditions lead to sure escape and some to safe capture. For example, a safe capture is guaranteed when the players' velocity vectors are parallel and P duplicates E's strategy.

The barrier is constructed as a semipermeable surface by means of the necessary conditions and the path equations of Section 3. Appropriate initial conditions are applied.

4.2. Initial Conditions for the Barrier. We shall look for a natural barrier, as defined by Isaacs. A natural barrier is tangent to the boundary C along the BUPs, in such a way that its normal ν coincides with the normal to C heading into the game space. Thus, a nonleaking barrier is guaranteed.

Using $\nu_0 = (-\sin\theta_0, -\cos\theta_0, 0)$ with (13) and (14), while the parameters of (11) are $s_1 = -1$ and $s_2 = \theta_0$, we obtain the barrier's initial switch functions on the BUPs,

$$A_0 = \nu_{\psi 0} = 0. \tag{16}$$

Now, using the first derivatives of the switch functions, and with the aid of (16), we get the optimal controls close to C (but not on it),

$$u^* = \sigma_1 = \text{sign } A = \text{sign } \mathring{A}_0 = \text{sign}(\sin\theta_0), \tag{17a}$$

$$v^* = \sigma_2 = \text{sign}(-\nu_\psi) = \text{sign}(-\mathring{\nu}_{\psi 0}) = \text{sign}[\sin(\theta_0 - \psi_0)]. \tag{17b}$$

Note that we have used the relationship $\mathring{A} = -\nu_x$.

We shall discuss two cases:

(i) $\theta_0 \neq 0$. We designate the right side ($\theta_0 < \pi$) by (+) and the left side ($\theta_0 > \pi$) by (−). The optimal controls (17) are $\sigma_1 \pm = -\sigma_2 \pm = \pm 1$ for a spiral BUP, and $\sigma_1 \pm = \sigma_2 \pm = \pm 1$ for a circular BUP. We shall examine, for example, the right-side cases.

On a right spiral BUP, we have

$$\mathring{r}_0 = 4\sin^2\theta_0/K > 0, \qquad \mathring{r}_0 = 0,$$

which means that the retrograde path goes outside the game space, and therefore is invalid.

On a right circular BUP, we have

$$r(\tau) = K, \qquad \psi(\tau) = 0,$$

which means that the retrograde path coincides with the BUP, and therefore is invalid too.

(ii) $\theta_0 = 0$. In this case, $\psi_0 = 0$ on both BUPs, and both switch functions in (17) are zero. We shall use the second derivatives to find the optimal controls near C,

$$u^* = \sigma_1 = \text{sign } \overset{\circ\circ}{A}_0 = \text{sign } \sigma_1, \tag{18a}$$

$$v^* = \sigma_2 = \text{sign}(-\overset{\circ\circ}{\nu}_\psi) = \text{sign } \sigma_2. \tag{18b}$$

These equations may render extremal controls, as well as zero controls (since the sign function is nondefined at zero). Thus, we have to check all nine possible combinations of controls (nine cases).

We shall use the following r-derivatives:

$$\overset{\circ}{r}_0 = \overset{\circ\circ}{r}_0 = 0, \tag{19a}$$

$$\overset{\circ\circ\circ}{r}_0 = \sigma_2^2 - \sigma_1^2, \tag{19b}$$

$$\overset{\circ\circ\circ\circ}{r}_0 = 3(\sigma_2 - \sigma_1)^2 / K. \tag{19c}$$

The possible combinations of controls are:

(a) $\sigma_1 = 0$, $\sigma_2 = \pm 1$ (two cases). Here, $\overset{\circ\circ\circ}{r}_0 = 1 > 0$; thus, the retrograde path goes outside the game space.

(b) $\sigma_1 = \sigma_2 = 0$ (one case). Here, there is no relative motion.

(c) $\sigma_1 = \sigma_2 = \pm 1$ (two cases). Here, $r(\tau) = K$ and $\psi(\tau) = 0$; thus, the retrograde path coincides with the circular BUP.

(d) $\sigma_1 = -\sigma_2 = \pm 1$ (two cases). Here, $\overset{\circ\circ\circ}{r}_0 = 0$, $\overset{\circ\circ\circ\circ}{r}_0 = 12/K > 0$, same as (a).

(e) $\sigma_1 = \pm 1$, $\sigma_2 = 0$ (two cases). Here, $\overset{\circ\circ\circ}{r}_0 = -1 < 0$, which means that the retrograde path goes inside the game space, and therefore these are the only valid candidates for initial controls on the barrier.

The optimal controls $\sigma_1 = \pm 1$ and $\sigma_2 = 0$ point out the existence of two singular paths of the type called evader's universal line (EUL). The EULs emanate from the point $(0, K, 0)$ to both directions determined by the sign of σ_1.

4.3. Typical Maneuvers on the Barrier. Tributary paths emanate (in retrograde time) from each EUL. A typical play starts on a tributary path, where each player turns right or left ($\sigma_1, \sigma_2 = \pm 1$), and continues on one of the EULs, P still turning and E moving straight ($\sigma_2 = 0$) on the tangent

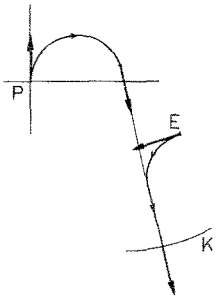

Fig. 3. Maneuver on the barrier, $\sigma_1 = 1$, $\sigma_2 = -1, 0$.

to both turn radii. Upon termination of the play, P completes his turn and is situated on the tangent, at a distance K behind E.

The set of all tributary paths composes the barrier's envelope. By symmetry, the barrier surfaces from the right side ($\sigma_1 = 1 \to \text{EUL}^+$) and the left side ($\sigma_1 = -1 \to \text{EUL}^-$) intersect at a pursuer's dispersal line (PDL). Beyond that intersection, all paths are discarded. It can be shown that, on the PDL, P is dominant. He has two options of turning direction, while E's direction is either unique or dependent on P's selection. There is also a region where E is dominant. This occurs on an evader's dispersal line (EDL), which will be discussed later.

Figure 3 presents a typical maneuver on the barrier. P is turning right, while E is turning left and then moving straight on the tangent to both turn radii.

Figure 4 shows a typical maneuver which starts on the PDL. Here, P has two options of turning, while E chooses a left turn and then a straight motion on the tangent to P's selected turn radius.

Figure 5 shows another PDL maneuver, with the difference that here E's turning direction is dependent on P's selection, such that $\sigma_2 = \sigma_1$. This

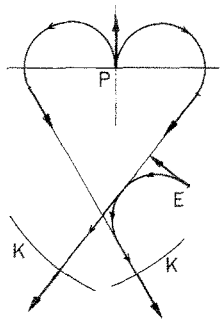

Fig. 4. Pursuer's dispersal point on the barrier, $\sigma_1 = \pm 1$, $\sigma_2 = -1, 0$.

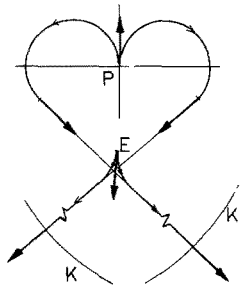

Fig. 5. Pursuer's dispersal point on the barrier, $\sigma_1 = \pm 1$, $\sigma_2 = \pm 1, 0$.

phenomenon was termed by Isaacs *instantaneous mixed strategy*. A slight difficulty arises, as E must have a small delay in his move, resulting from the lack of information as to his opponent's current control. This drives E off the barrier into the capture zone and necessitates the redefinition of the barrier as a semipermeable surface, located at an infinitesimal distance off the original barrier, in the escape zone.

Figure 6 demonstrates a typical maneuver which starts on the EDL. Here, E has two options of turning, while P chooses his direction dependently, in such a way that $\sigma_1 = \sigma_2$. The same difficulty arises as before with a similar treatment. This EDL relates to the phenomenon termed by Isaacs the *perpetuated dilemma*, in view of the fact that E can delay his decision along it.

4.4. Analytical Solution of the Barrier's Equations. Using the general path equations of zero control for E (15) and the initial conditions of Section 4.2, we may write the equations of the EULs:

$$x = \sigma_1[(K - \tau)\sin\tau + 1 - \cos\tau], \tag{20a}$$

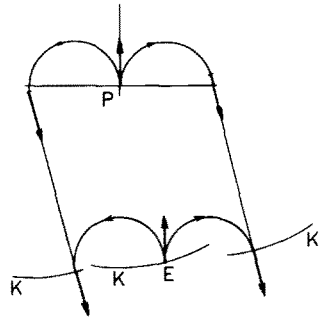

Fig. 6. Evader's dispersal point on the barrier, $\sigma_1 = \pm 1$, $\sigma_2 = \pm 1$.

$$y = (k - \tau)\cos\tau + \sin\tau, \tag{20b}$$

$$\psi = \sigma_1 \tau. \tag{20c}$$

We take the EUL's equations (20) as a set of initial conditions at time τ_1, and substitute them into the general path equations (12) to obtain the tributaries. Then, we eliminate τ_1 to get the barrier equations,

$$x = x(\psi, \tau) = [K - \sigma_1\psi + (1 - \sigma_1\sigma_2)\tau]\sin(\psi + \sigma_2\tau) - (\sigma_1 - \sigma_2)\cos(\psi + \sigma_2 t) - \sigma_2\cos\psi + \sigma_1, \tag{21a}$$

$$y = y(\psi, \tau) = [K - \sigma_1\psi + (1 - \sigma_1\sigma_2)\tau]\cos(\psi + \sigma_2\tau) + (\sigma_1 - \sigma_2)\sin(\psi + \sigma_2\tau) + \sigma_2\sin\psi, \tag{21b}$$

while τ_1 is

$$\tau_1 = \sigma_1\psi - (1 - \sigma_1\sigma_2\tau). \tag{22}$$

Remark. For the case $\sigma_1 = \sigma_2$, the tributaries have a constant ψ, and (21) are circles of radius $K - |\psi|$ with center at

$$x = \sigma_1(1 - \cos\psi), \qquad y = \sigma_1 \sin\psi.$$

In (21) and (22), τ_1 is the retrograde time of motion on EUL, and τ is the retrograde time of motion on the tributary. The total time of a play is $\tau_t = \tau + \tau_1$.

Equations (21) represent the barrier surfaces on the right ($\sigma_1 = 1$) and on the left ($\sigma_1 = -1$). We can display cross sections of constant ψ through the barrier, using the parameter τ and the appropriate values of $\sigma_{1,2}$. We have four strategy regions a, b, c, d, as defined on Fig. 7.

We designate by $(+)$ the right-side values and by $(-)$ the left-side values. We use (21) to equate both sides, on the line of intersection between them, to obtain the barrier

$$x(\psi^+, \tau^+; \sigma_2^+) = x(\psi^-, \tau^-; \sigma_2^-), \tag{23a}$$

$$y(\psi^+, \tau^+; \sigma_2^+) = y(\psi^-, \tau^-; \sigma_2^-). \tag{23b}$$

Remark. The numerical values of $\psi^{\pm}$ should maintain $0 \leq \psi^+ \leq 2\pi$ and $-2\pi \leq \psi^- \leq 0$.

Equations (23) represent four combinations of σ_2^+ and σ_2^-, of which only three practically exist.

Eliminating τ^+ and τ^- from (23), then using the relationship $\psi^- = \psi^+ - 2\pi$ (at a common ψ-cross section), and substituting the appropriate values of σ_2^+ and ψ_2^-, we get the equations of the PDL,

$$x = x[\psi, \tau(\psi)] = x(\psi), \tag{24a}$$

$$y = y[\psi, \tau(\psi)] = y(\psi). \tag{24b}$$

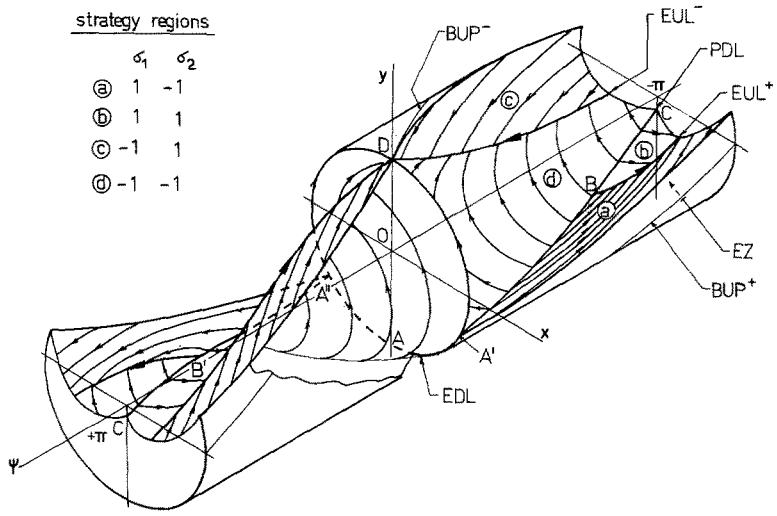

Fig. 7. Schematic description of the barrier in the state space, $-\pi \leq \psi \leq \pi$, $K \geq \pi + 2$.

A numerical solution is mandatory for the transcendental equations (23). While solving them, the values of σ_2^+ and σ_2^- are selected in such a way that (22) shall always yield $\tau_1^{\pm} \geq 0$.

It is to be mentioned that, in the GOK, the total time to termination, from both sides of the PDL, is not the same, meaning $\tau_t^+ \neq \tau_t^-$.

4.5. Description of the Barrier. The construction described above yields a closed barrier for $K \geq \pi + 2$ (K is the ratio of the surveillance radius to the minimal turn radius). It can be shown that, for $K < \pi + 2$, the left and right wings of the barrier, constructed in Section 4.4, do not fully intersect, and thus are leaking. Since we conjecture that a closed barrier exists in this game, a different method of construction for $K < \pi + 2$ should be applied. This is left for further research.

Using the equations of the gradient of the value (13) and the switch functions (14), with the appropriate initial conditions from Section 4.2 and Eqs. (20), it can be shown that, for $K \geq \pi + 2$, no switching occurs along the EULs or the tributaries. This confirms the validity of the analysis.

Figure 7 depicts schematically the barrier in the state space for $K \geq \pi + 2$, in the region $-\pi \leq \psi \leq \pi$, with the capture zone removed. Note that $\psi = \pi$ and $\psi = -\pi$ is identical.

We shall now describe the barrier.

The EULs terminate at point $D(0, K, 0)$. $\text{EUL}^+(\text{DB})$ represents a right turn for P, and $\text{EUL}^-(\text{DB}')$ represents a left turn for P. The tributaries from

each side of each EUL represent a right turn or a left turn for E. The surfaces of tributaries form the barrier. The resulting strategy regions are designated a, b, c, d.

We have tributaries of the type $\sigma_1 = \sigma_2$, with constant ψ and a circular shape, and tributaries of the type $\sigma_1 = -\sigma_2$, with time-changing ψ and a complicated geometry. The barrier intersects the boundary C slightly above the spiral BUPs. At $\psi = 0$, it coincides with the circular BUPs. The barrier is not tangent to C anywhere except at point D.

The intersection of the right and left surfaces of tributaries creates the PDL. The EULs touch the PDL at points B and B', on which one of the options for E is a straight line motion (depending upon P's decision). Along the section BB' of the PDL, the typical maneuvers are as in Fig. 5. Along the sections $A'B$ and $A''B'$, the maneuvers are similar to Fig. 4. Thus, we have the following strategy combinations on the PDL: a-d, b-d, b-c (a-c does not exist). For example, b-d exists in Fig. 5, and a-d in Fig. 4. The PDL intersects the boundary at points A' and A'', and not at $A(0, -K, 0)$, as might be expected from symmetry. The circular arc $A'AA''$ is the EDL (evader's dispersal line), which separates two regions of different strategies for both P and E.

Figures 8 and 9 depict ψ-cross sections through the barrier in the state space for $K = 6$ and $K = \pi + 2$ in the region $-\pi \leq \psi \leq 0$. These figures were obtained by computing the barrier equations (21) and finding the PDL graphically. In both figures, lines with arrows indicate tributaries in a real view ($\sigma_1 = \sigma_2$), and lines without arrows indicate cross-sections through tributaries ($\sigma_1 = -\sigma_2$). The PDL, EUL, and the strategy regions are indicated

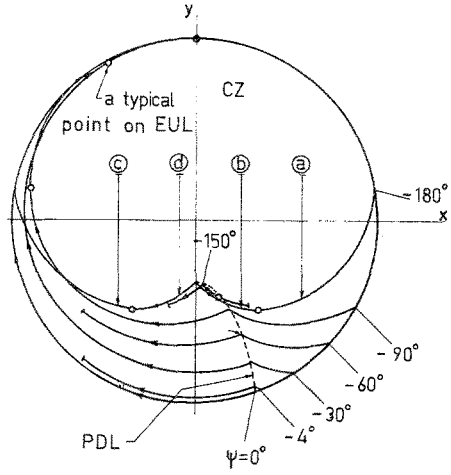

Fig. 8. ψ-cross sections of the barrier, $K = 6$, $-\pi \leq \psi \leq 0$.

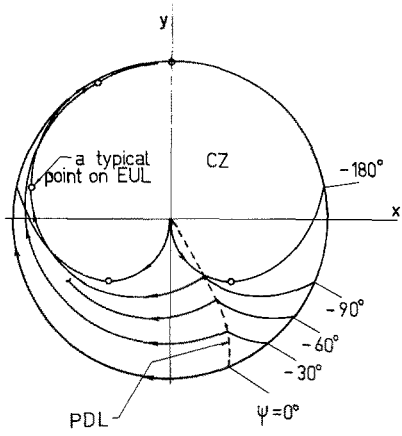

Fig. 9. ψ-cross sections of the barrier, $K = \pi + 2$, $-\pi \leq \psi \leq 0$.

on the figures. The region $0 \leq \psi \leq \pi$ can be depicted using symmetry around the axis y.

The barrier attained is smooth, except on the PDL. As K is growing bigger, the escape zone is smaller and the capture zone bigger. At $K > 100$, the escape zone becomes a nonsignificant portion of the game space.

The case $K = 6$ in Fig. 8 is typical: EUL^+ exists up to $\psi \cong -138.5°$ at point B of Fig. 7. The PDL starts at point $C(0, -2.04, -\pi)$ and ends on the boundary at point $A'(2.1, -5.7, 0)$. The value $X \cong 2$ is typical. We can see that the barrier intersects the boundary above the spiral BUPs and that, at $\psi = 0$, it coincides with the circular BUP. At this region, the barrier is not tangent to the boundary, as may be seen if we take a θ cross section through the game space.

The case $K = \pi + 2$ in Fig. 9 represents the smallest K possible for our method of barrier construction. It can be seen that the tributaries at $\psi = -\pi$ are tangent to each other at the point $(0, 0, -\pi)$. A smaller K will cause the opening of the barrier at this point and its vicinity. Depicting the real space maneuvers at this point reveals its uniqueness. The critical value $K = \pi + 2$ may be obtained by substituting $\psi = \pi$ into the tributary equations (21) with $\sigma_1 = \sigma_2$.

5. Game of Degree (GOD)

5.1. General Concepts. In the GOD, we look for optimal strategies and paths in the escape zone EZ. We use the necessary conditions and the path equations of Section 3. Appropriate initial conditions are applied on the usable part.

The method of solution is somewhat similar to that of the GOK; but, due to higher dimensionality, it is more complicated. Here too, the solution is valid for $K \geq \pi + 2$ only.

5.2. Initial Conditions. Since the GOD is a game with integral payoff, ∇T_0 is codirectional with ν_0. With the aid of ME2 (7), we obtain on the usable part the parameters of (11),

$$s_1 = 1/[\cos\theta_0 - \cos(\psi_0 - \theta_0)], \qquad s_2 = \theta_0, \qquad T_{\psi 0} = 0.$$

Thus, in a similar way to Section 4.2, we find that the initial switch functions are zero [as in (16)], and that the optimal controls near the boundary C are the same as in (17). The controls in (17) switch on the UP at $\theta_0 = \pi$ (for σ_1) and at $\theta_0 = \psi_0$ (for σ_2). Thus, the sign regions on the UP are

$$\sigma_1 = 1\colon\ 0 < \theta_0 < \pi, \qquad \sigma_2 = 1\colon\ \psi_0 < \theta_0 < 2\pi; \tag{25a}$$

$$\sigma_1 = -1\colon\ \pi < \theta < 2\pi, \qquad \sigma_2 = -1\colon\ 0 < \theta_0 < \psi_0. \tag{25b}$$

On the switch lines $\theta_0 = \pi$ and $\theta_0 = \psi_0$, we examine the second derivatives of the switch functions near C. Thus, we have

$$u^* = \sigma_1 = \operatorname{sign} \overset{\circ\circ}{A}_0 = -\operatorname{sign} \sigma_1, \qquad \theta_0 = \pi, \tag{26a}$$

$$v^* = \sigma_2 = \operatorname{sign}(-\overset{\circ\circ}{T}_{\psi 0}) = \operatorname{sign} \sigma_2, \qquad \theta_0 = \psi_0, \tag{26b}$$

The equation of σ_2 indicates the existence of an evader's universal surface (EUS), emanating from the line $\theta_0 = \psi_0$ on C. The equation of σ_1 indicates the existence of a pursuer's dispersal surface (PDS), emanating from the line $\theta_0 = \pi$ on C. Note that this equation is not valid for $\sigma_1 \neq 0$. The identity of each singularity may be verified by examining the velocity vectors at both sides of each switch line, to be either dispersive or convergent.

Figure 10 summarizes the initial conditions on a spreading of C. The strategy regions are designated by the letters a to d, in correlation with the regions in the GOK (Fig. 7). In Fig. 10, $(+)$ designates right side $(\sigma_1 = 1)$ and $(-)$ designates left side $(\sigma_1 = -1)$.

5.3. Typical Maneuvers in the GOD. Differently from the GOK, in the GOD we have both paths emanating (in retrograde time) from the usable part UP and paths emanating from the universal surfaces EUS (the tributaries). Thus, a part of the pursuits terminate by moving on the EUS, E moving in a straight line and P still turning at the moment of termination. The other part of the pursuits terminate on the UP directly, both players still turning at the moment of termination. At termination, E escapes.

By symmetry, optimal paths from the right side $(\sigma_1 = 1)$ and the left side $(\sigma_1 = -1)$, from both types, EUS's and UP's, intersect on points of

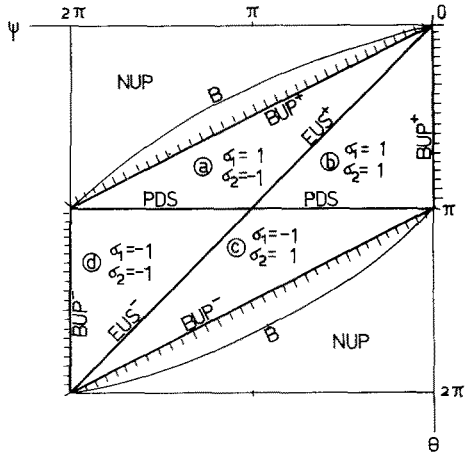

Fig. 10. Initial strategies on the usable part.

equal time to termination τ_t (the value $T = \tau_t$) for both directions of motion. The set of all these points forms the pursuer's dispersal surface PDS. The paths beyond the PDS are discarded. As in the GOK, P is dominant on the PDS, and E's maneuvers are dependent.

Figure 11 shows a typical maneuver which terminates on the UP. P is turning left, while E is turning left. At termination (escape), the distance between the players is K, and both are still turning.

Figure 12 shows a typical maneuver which includes motion on the EUS. P is turning right, while E is turning left and then moving straight,

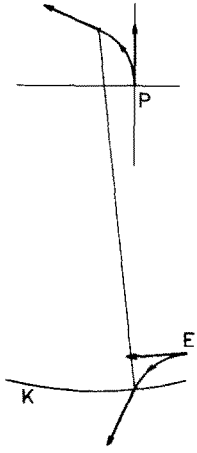

Fig. 11. Maneuver terminating on the usable part in the game of degree, $\sigma_1 = -1$, $\sigma_2 = -1$.

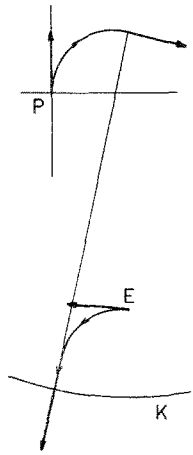

Fig. 12. Maneuver terminating on the evader's universal surface in the game of degree, $\sigma_1 = 1$, $\sigma_2 = -1, 0$.

on the line which goes through P's point of termination and is tangent to E's turning radius.

The variety of types of paths and strategy regions composes the various sections of the PDS. Two examples follow.

Figure 13 shows a typical maneuver which starts on the PDS. Both options of P lead to termination on the UP directly. It is interesting to see that, in this case, $\theta_0^+ = \theta_0^-$ (this fact may be derived analytically).

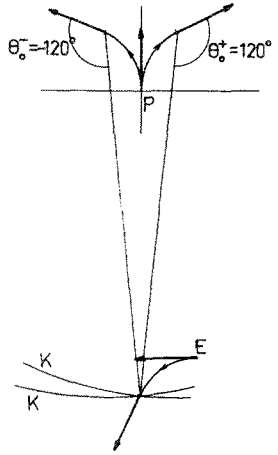

Fig. 13. Pursuer's dispersal point in the game of degree, $\sigma_1 = \pm 1$, $\sigma_2 = -1$.

Figure 14 shows another PDS maneuver, whereby a right turn for P leads to an EUS type of termination (E moving straight), while a left turn for P leads to termination on the UP directly.

While, in the cases of Figs. 13 and 14, E's direction of turning is unique (as in Fig. 4 of the GOK), a case where E's direction depends on P's selection is also possible (as in Fig. 5 of the GOK).

5.4. Analytical Solution of the GOD. As in the GOK, we may use the general path equations for $\sigma_2 = 0$ [Eq. (15)] and the initial conditions of Section 5.2 to get the equations of the EUSs. Those equations serve as sets of initial conditions at time τ_1 for the tributaries. We substitute them into the general path equations (12) and eliminate τ_1. We use the total time of an optimal play (the value) $\tau_t = \tau + \tau_1$, where τ_1 is motion on EUS and τ is motion on the tributary. Thus, we have the following tributary equations:

$$x = x(\psi, \tau_t, \theta_0) = [K + \sigma_2(\theta_0 - \psi) - (1 - \sigma_1\sigma_2)\tau_t] \sin(\theta_0 + \sigma_1\tau_t)$$
$$+ \sigma_2[\cos(\theta_0 + \sigma_1\tau_t) - \cos\psi] + \sigma_1(1 - \cos\tau_t), \tag{27a}$$

$$y = y(\psi, \tau_t, \theta_0) = [K + \sigma_2(\theta_0 - \psi) - (1 - \sigma_1\sigma_2)\tau_t] \cos(\theta_0 + \sigma_1\tau_t)$$
$$- \sigma_2[\sin(\theta_0 + \sigma_1\tau_t) - \sin\psi] + \sin\tau_t. \tag{27b}$$

Using the general path equations (12), with initial conditions on the UP from Section 5.2, then eliminating ψ_0 and using $\tau_t = \tau$, we obtain the

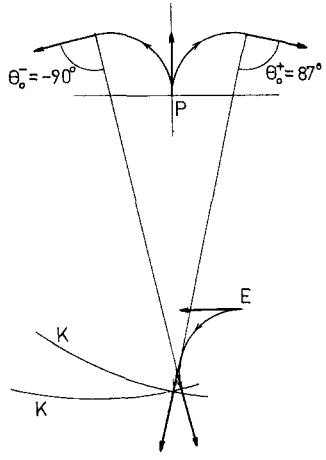

Fig. 14. Pursuer's dispersal point in the game of degree, $\sigma_1 = \pm 1$, $\sigma_2 = -1, 0$.

following UP paths equations (paths terminating directly on UP):

$$x = x(\psi, \tau_t, \theta_0) = K \sin(\theta_0 + \sigma_1\tau_t) + \sigma_1(1 - \cos\tau_t) + \sigma_2[\cos(\psi + \sigma_2\tau_t) - \cos\psi], \tag{28a}$$

$$y = y(\psi, \tau_t, \theta_0) = K \cos(\theta_0 + \sigma_1\tau_t) + \sin\tau_t - \sigma_2[\sin(\psi + \sigma_2\tau_t) - \sin\psi]. \tag{28b}$$

Also, we have the relationships

$$\tau_1 = -\sigma_2(\theta_0 - \psi) + (1 - \sigma_1\sigma_2)\tau_t, \tag{29a}$$

$$\psi_0 = \psi - (\sigma_1 - \sigma_2)\tau_t. \tag{29b}$$

Remark. In (27) and (28), we could eliminate ψ_0, instead of θ_0 or τ_1, but it proves to be inconvenient.

Equations (27) and (28) represent the optimal paths, both those emanating directly from the UP and those emanating from the EUSs, on the right side ($\sigma_1 = 1$, designated by $+$) and on the left side ($\sigma_1 = -1$, designated by $-$). On the whole, we have $2^3 = 8$ types of trajectories. We shall designate them by two letters, the first letter stands for the sign region a, b, c, d (defined in Figs. 10 and 15); and the second letter is U (for UP) and E (for EUS). For example, bE is an EUS-tributary with $\sigma_1 = \sigma_2 = 1$.

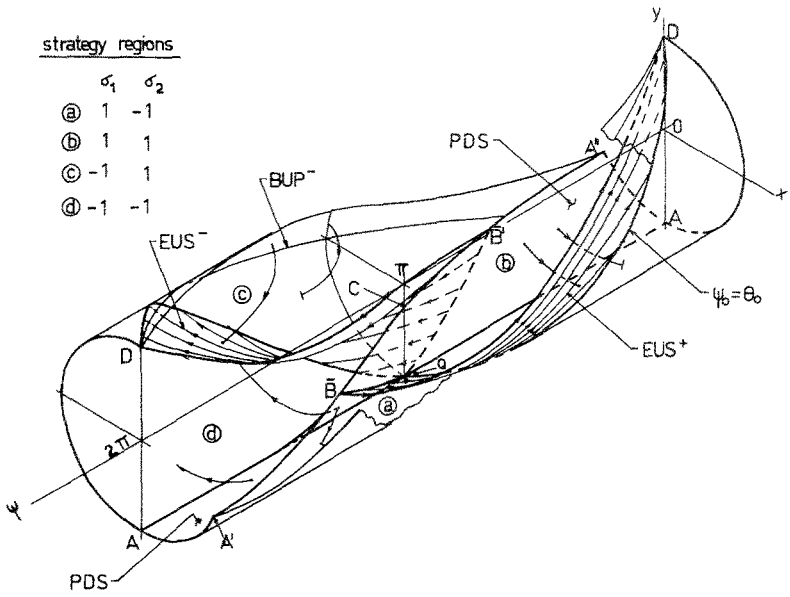

Fig. 15. Schematic description of the game of degree in the state space, $2\pi \leq \psi \leq 0$, $K \geq \pi + 2$.

We can display cross sections of constant ψ through the paths, in the state space, using the parameters τ_t and θ_0, and the appropriate values of $\sigma_{1,2}$.

The paths from both sides meet on the PDS at points of equal value $T = \tau_t$. On the point of intersection, we may use Eqs. (27) and (28) to equate both sides,

$$x(\psi^+, \tau_t^+, \theta_0^+; \sigma_2^+) = x(\psi^-, \tau_t^-, \theta_0^-; \sigma_2^-), \tag{30a}$$

$$y(\psi^+, \tau_t^+, \theta_0^+; \sigma_2^+) = y(\psi^-, \tau_t^-, \theta_0^-; \sigma_2^-). \tag{30b}$$

Remark. The numerical values of θ_0 and ψ should maintain $0 \leq \theta_0^+$, $\psi^+ \leq 2\pi$ and $-2\pi \leq \theta_0^-$, $\psi^- \leq 0$.

Equations (30) represent $(2^2)^2 = 16$ combinations of $U_P^{\pm}$-paths, EUS$^{\pm}$-tributaries, and $\sigma_2^{\pm}$, of which only 12 practically exist. A maximum of four combinations exists at a specific ψ-cross section. For example, the combination aU$-$cE stands for a dispersal point created by the intersection of a UP-path with $\sigma_1 = -\sigma_2 = 1$ and an EUS-tributary with $\sigma_1 = -\sigma_2 = -1$. Figure 13 represents the combination aU–dU. Figure 14 represents the combination aE–dU.

Using the equality of the value on the PDS ($\tau_t = \tau_t^+ = \tau_t^-$), and the relationships $\psi^- = \psi^+ - 2\pi$ and $\theta^- = \theta^+ - 2\pi$ (at an arbitrary point in the game space), then substituting the appropriate values of σ_2^+ and σ_2^-, and eliminating θ_0^+ and θ_0^-, we have the equations of the PDS,

$$x = x[\psi, \tau_t, \theta_0(\psi, \tau_t)] = x(\psi, \tau_t), \tag{31a}$$

$$y = y[\psi, \tau_t, \theta_0(\psi, \tau_t)] = y(\psi, \tau_t). \tag{31b}$$

A numerical solution is mandatory for the transcendental equations (30), except for combinations of the type *U–*U. While solving numerically, the values of σ_2^+ and σ_2^- and the appropriate combinations are selected in such a way that (29) shall always yield $\tau_1^{\pm} \geq 0$ (for UP-paths) and $\sigma_2\psi_0 < \sigma_2\theta_0$ (for EUS-tributaries).

5.5. Description of the Paths and the Singular Surfaces in the GOD. As mentioned before, the solution of the GOD presented here is valid for $K \geq \pi + 2$ only, for which a closed barrier was ascertained. The complementary region awaits another research.

We use the equations of ∇T [Eqs. (13)] and the switch functions (14), for both UP-paths and EUS-tributaries, with the initial conditions of Section 5.2, to examine the possibility of further switching of controls. Though we conjecture that no further switching occurs for $K \geq \pi + 2$, it is impossible

to prove it analytically, the equations being transcendental. Thus, each case should be verified numerically to support this conjecture. The cases that we have checked comply with it.

Figure 15 depicts schematically the singular surfaces and optimal paths of the GOD, for $K \geq \pi + 2$, in the region $0 \leq \psi \leq 2\pi$, with the capture zone and the barrier removed. Note that $\psi = 0$ and $\psi = 2\pi$ is identical.

We shall now describe the GOD.

The PDS divides the escape zone EZ into a region of right turns for P and a region of left turns for P. These two regions are again divided, each by the relevant EUS, into regions of right turns for E and regions of left turns for E. The four regions were designated a, b, c, d according to Fig. 15.

The four regions are filled with optimal paths, which start (in real time) on the PDS, or on the nonusable part (NUP), or close to the barrier. Some of them are EUS-tributaries, and some terminate directly on the UP. As in the GOK, paths of $\sigma_1 = \sigma_2$ (regions b and d) are ψ-constant.

Paths of the various types are shown, as examples, on Fig. 15. The EUSs themselves consist of optimal paths of the type EUL, that start on the PDS or close to the barrier, and terminate on the UP along the line $\psi_0 = \theta_0$. EUS$^+$'s borders are DQ along the UP, $D\bar{B}$ along the barrier, EUS$^-$ and BQ along the PDS. EUS$^-$ goes symmetrically. On the EUSs, E moves in a straight line.

The PDS's borders are the line AQA on the boundary C, the arcs AA' and AA'', and the line $A'CA''$ on the barrier. The intersection of the PDS with the barrier is close to the PDL, but does not coincide with it, except in points A', A'', C of Fig. 7 and Fig. 15. This is due to the differences in times to terminations, which is the result of the different definition of the payoff in the GOK and the GOD. EUSs, though, intersect the barrier at the EUL's of the barrier (lines $D\bar{B}$ and $D\bar{B}'$) up till the PDS or the PDL (as applicable).

In fact, no paths of the GOD, including paths on the EUS, intersect the barrier, but rather thay come very close. There is a discontinuity in ∇T across the barrier.

On the PDS, P has two options of heading. As in the GOK, on one region of the PDS (the surface $\bar{B}Q\bar{B}'$) E's control depends on P's decision (combination b*-d*), and on the other two regions of the PDS, E's control is unique (combinations a*-d* and b*-c*). A combination aU-dE is shown, as an example, on Fig. 15.

Figures 16 to 20 present various ψ-cross sections of constant θ_0 through the state space of the GOD, in the region $-\pi \leq \psi \leq 0$, for $K = 6$. These figures were obtained by computing the path equations (27) and (28) and by finding the PDS graphically, by means of isochrones (lines of constant time to termination τ_t). Isochrones from right and from left, having the

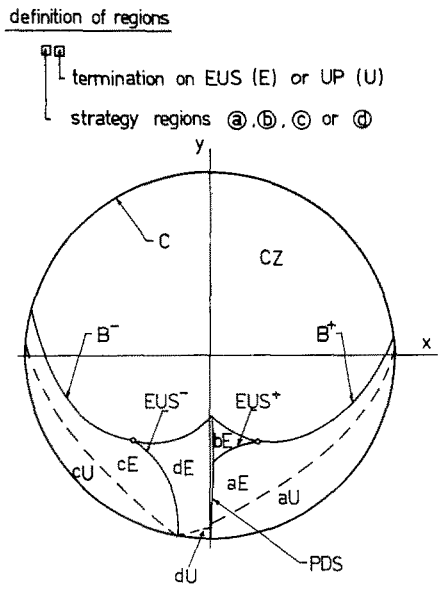

Fig. 16. Typical ψ-cross section through the singular surfaces in the game of degree, $-\pi \leq \psi \leq 0$, $K \geq \pi + 2$.

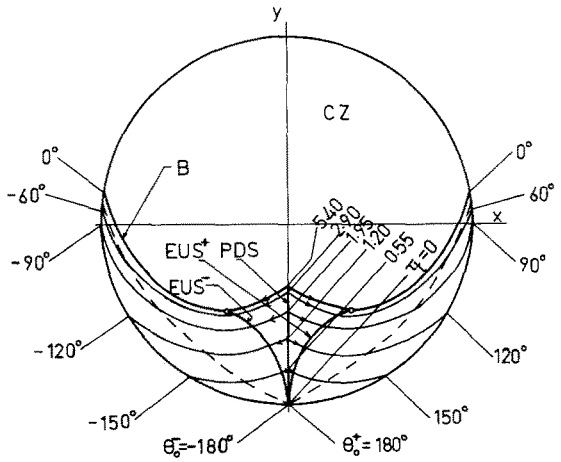

Fig. 17. ψ-cross sections of constant θ_0 in the game of degree, $K = 6$, $\psi = -180°$.

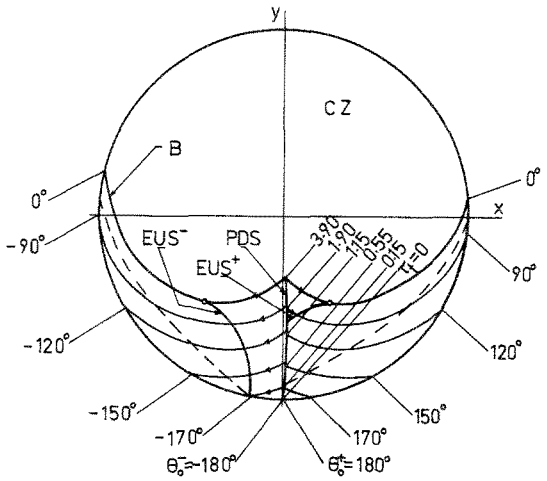

Fig. 18. ψ-cross sections of constant θ_0 in the game of degree, $K=6$, $\psi=-170°$.

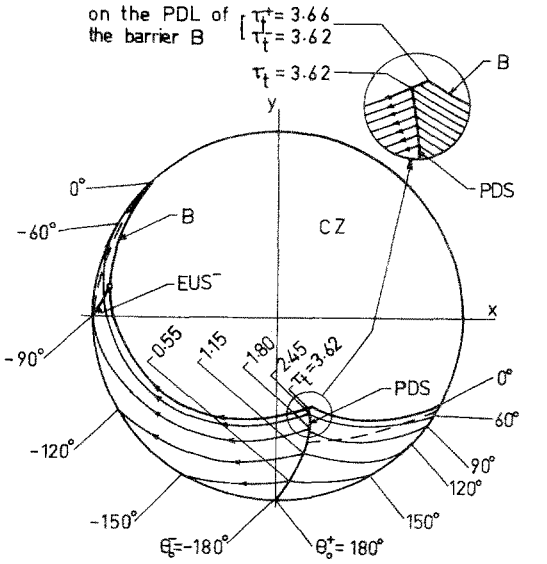

Fig. 19. ψ-cross sections of constant θ_0 in the game of degree, $K=6$, $\psi=-90°$.

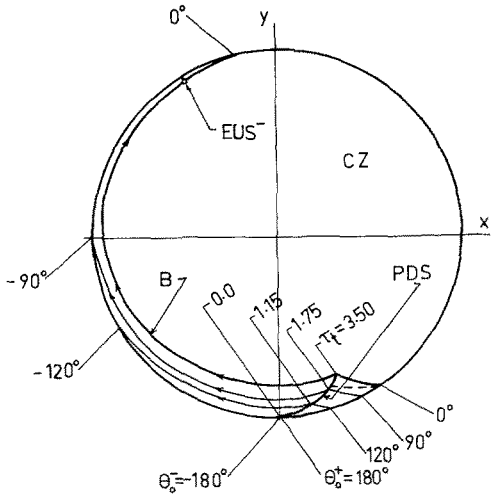

Fig. 20. ψ-cross sections of constant θ_0 in the game of degree, $K = 6$, $\psi = -30°$.

same τ_t, were intersected to yield the PDS. The isochrones were computed by (27) and (28), taking τ_t constant and varying the parameter θ_0.

Figure 16 shows a typical ψ-cross section through the escape zone and the singular surfaces. The various types of regions are noted, using the notation of this section. It may be noticed that the PDS, in this case, consists of the combinations aU-dU, aU-dE, aE-dE, and bE-dE. Note also that a bU type of path does not exist in this cross section.

Figure 18 is a full representation of Fig. 16, $\psi = -170°$. Here, paths in a real view (regions of $\sigma_1 = \sigma_2$) are indicated by arrows, and the lines without arrows (in regions of $\sigma_1 = -\sigma_2$) are cross sections through paths of constant θ_0. τ_t is indicated on some points of the PDS. Note that, except for the combination aU-dU, lines of equal $|\theta_0|$ do not meet at the same point on the PDS (though quite close to each other, in this case).

Figure 17 depicts the symmetric case $\psi = -180°$. Here, the cross section of the PDS is a straight line, created by the single combination bE-dE.

Figure 19 shows the case $\psi = -90°$. Here, the EUS^+ vanishes completely, and the PDS's combinations are aU-dU, aE-dU (a new one), and aE-dE. This case shows clearly that the PDS slightly deviates from the PDL on the barrier, and the difference in τ_t is indicated.

Figure 20 shows the case $\psi = -30°$. Here, the PDS-cross section is approaching the circular BUP.

Note on the numerical solution. Due to the variety of combinations, and due the absence of preinformation as to the border surfaces dividing

the various regions, the numerical solution is complicated, and full automation of the computations seems not to be feasible. Thus, the construction is done step-by-step, at each step verifying the absence of switching, the validity of Eqs. (29), and the borders of the current region. The PDS is plotted either graphically or by solving a set of two transcendental equations (30) with two independent variables.

6. Composite Game of Two Identical Cars

This research is the complementary problem of the game of pursuit and evasion solved by Merz (Ref. 2). The two problems are dual, but still each is unique. They both use identical dynamics. In the game of pursuit and evasion (GPE), the game space is outside the radius K, and P minimizes while E maximizes the time to capture. In the game of surveillance-evasion (GSE), the game space is inside K, and P maximizes while E minimizes the time to escape. Thus, the players' objectives in the two games are contrary. This duality continues with contrary optimal control functions, with substitution of the typical maneuvers and singular surfaces between the players, and other features.

The uniqueness of the GSE starts with the barrier construction. The barrier is not a *natural barrier*, as opposed to the GPE, because it is not tangent to the BUPs. Thus, we have in the GSE paths that start on the nonusable part (NUP). Also, all the paths on the barrier terminate on the EUL, E moving straight. The GSE holds an additional singular phenomenon of the type, called the perpetuated dilemma, which is a dispersal surface for E.

Maybe the most interesting is the sensitivity of the GSE to changes in the parameter K. Though we conjecture that a closed barrier exists in the GSE, our construction holds only for $K \geq \pi + 2$, whereas a different method, probably more complicated, should be applied for $K < \pi + 2$. In the GPE, the same method of constructions holds for all values of K.

Figure 21 summarizes some of the properties of the GPE and the GSE on a common ψ-cross section of the game space. In that figure, entities of the GSE are designated by the index e, and those of the GPE by p. For example, PUS$\bar{\text{p}}$ is a left pursuer's universal surface in the GPE.

A composite game of two identical cars, incorporating the GPE and the GSE together, may be synthesized. The concept of such a game maintains that all the 2-D realistic space is measurable for the state vector and that P is striving to gain surveillance over E inside the region of radius K. In such a game, the various sections of the boundary C are singular surfaces of various types, and definition of barriers is needed. For example, a path

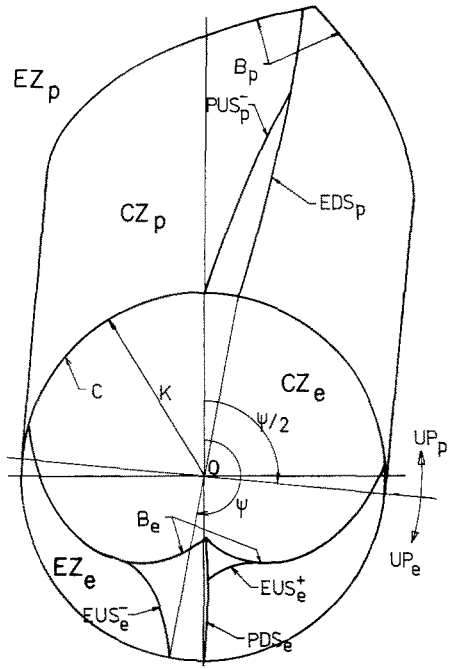

Fig. 21. Schematic ψ-cross section in the composite game of two identical cars, $K \geq \pi + 2$.

starting in the escape zone of the GSE (EZ_e) leads always to the escape zone of the GPE (EZ_p). But a path starting in the capture zone of the GPE (CZ_p) leads sometimes to the escape zone of the GSE (EZ_e). This may be an interesting problem for further research.

7. Conclusions

The problem of surveillance-evasion in the dynamics of two identical cars turns out to be an interesting and intriguing duality to the problem of pursuit and evasion of the same dynamics.

This work presents a full solution of the problem, in the region $K \geq \pi + 2$. The solution includes the construction of a closed barrier and definition of the strategy regions, singular entities and optimal paths, on the barrier and inside the escape zone. Some unique features of the game were discussed.

It seems worthwhile to pursue further research for the region $K < \pi + 2$, for which the solution does not hold. This region of K represents cases of

small surveillance radius and large turn radii, which may be applicable to some practical problems like collision avoidance.

A generalization of the game of two identical cars may be obtained by uniting the game of surveillance-evasion and the game of pursuit and evasion. This may cover fully the problem of surveillance. Also, other kinds of surveillance zone geometries, like conic surveillance zone, may be used with the same dynamics.

References

1. GREENFELD, I., *A Differential Game of Surveillance Evasion in the Model of Two Identical Cars*, Faculty of Mechanical Engineering, Technion, Haifa, MS Thesis, 1983.
2. MERZ, A. W., *The Game of Two Identical Cars*, Journal of Optimization Theory and Applications, Vol. 9, No. 5, 1972.
3. DOBBIE, J. M., *Solution of Some Surveillance-Evasion Problems by the Methods of Differential Games*, Proceedings of the 4th International Conference on Operational Research, MIT, John Wiley and Sons, New York, New York, 1966.
4. LEWIN, J., and BREAKWELL, J. V., *The Surveillance-Evasion Game of Degree*, Journal of Optimization Theory and Applications, Vol. 16, Nos. 3/4, 1975. 1975.
5. LEWIN, J., and OLSDER, G. J., *Conic Surveillance-Evasion*, Journal of Optimization Theory and Applications, Vol. 27, No. 1, 1979.
6. ISAACS, R. P., *Differential Games*, 2nd Edition, John Wiley and Sons, New York, New York, 1975.